Small-Signal Analysis of 1.3-μm Microcavity Light-Emitting Diodes

P. Landais, B. Roycroft, A. Shaw, B. Depreter, I. Moerman, *Member, IEEE,* and J. Hegarty, *Member, IEEE*

Abstract— **The modulation speed of 1.3-μm microcavity light-emitting diodes (MCLED's) has been measured using a small-signal modulation analysis. A speed of 260 MHz using a 25-μm diameter sample at current density of 10 kA/cm^2 has been achieved. The carrier confinement has been calculated for several carrier densities in order to investigate the origin of the speed limitation. By comparing the performance of the 1.3-μm MCLED's with that of the 990-nm devices we conclude that the limiting factor on the speed seems to be a lack of carrier confinement in the quantum wells and not a cavity effect.**

Index Terms— **Communication systems, frequency response, light-emitting diodes, microcavity, quantum-well devices.**

I. Introduction

PLANAR microcavity light-emitting diodes (MCLED's) are formed by a vertical Fabry–Perot cavity containing an active layer. In the "weak coupling" regime, the fundamental mode of the confined dimension of the cavity corresponds to the emission peak wavelength of the active medium. This interference effect selects the emitted mode, increases its power at the expense of the other modes and modifies its spatial distribution. Consequently, MCLED's feature an increase of the extraction efficiency, of the directionality of the emission and a narrowing of the emission spectrum [1]–[4]. These advantages over standard light emitting diodes make the MCLED's very attractive for applications such as lighting [5], interconnects [6], gas sensing [7], and for fiber-optic communication at $\lambda = 0.65\,\mu$m [8] and from $\lambda = 0.85$ to $\lambda = 1.5\,\mu$m [9], [10]. Though 1.3-μm MCLED's have already been demonstrated [10]–[12] there has been no report to date of their amplitude modulation (AM) speed, a parameter of special importance in many applications at $\lambda = 1.3\,\mu$m. The purpose of this paper is to evaluate the modulation performance of the state-of-art 1.3-μm MCLED's and to investigate whether the use of a micro-cavity design introduces any limitations of the operating speed compared to conventional LED's. Reduction of the speed could occur as a result of photon recycling, a mechanism which has been inferred in MCLED operating at $\lambda = 990$ nm [13]. We present the dependence of the small-signal bandwidth with bias current for a 1.3-μm MCLED. Sample fabrication is described in the next paragraph, after which the experimental setup is introduced. Finally the results achieved are presented and discussed. They show that the dominant effect in the limitation of the bandwidth (BW) is the lack of carrier confinement and not any cavity effect such as photon recycling.

Manuscript received April 14, 1999; revised August 2, 1999. This work was supported by European Contract ESPRIT SMILED 24997.

P. Landais is with Optronics Ireland, Physics Department, Trinity College Dublin, Dublin 2, Ireland.

B. Roycroft, A. Shaw, and J. Hegarty are with the Physics Department, Trinity College Dublin, Dublin 2, Ireland.

B. Depreter and I. Moerman are with the University of Gent-IMEC, INTEC Department, B-9000 Gent, Belgium.

Publisher Item Identifier S 1041-1135(99)08678-4.

II. Device Structure And Fabrication

The components under test are 1.3 μm substrate emitting MCLED's. Their structure is a planar λ-scale Fabry–Perot cavity containing three $In_{0.75}Ga_{0.25}As_{0.8}P_{0.2}$/InP quantum wells (QW's), grown by metal-organic chemical vapor deposition. The epitaxial growth was performed in two steps on an n-type InP substrate allowing precise positioning of the QW's with respect to the cavity resonance. In the first growth step, the n-doped distributed Bragg reflector (DBR) consisting of 15-pairs of $In_{0.75}Ga_{0.25}As_{0.54}P_{0.46}$–InP layers was grown at low pressure. In the second step, the active layers and the p-type layers were grown. Growth of the p-type layers under atmospheric pressure permits a better incorporation of the Zn doping. The top mirror is a 200-nm evaporated layer of Au which also acts as a p-type contact. A circular mesa was etched to ensure current confinement. The n-type contact consists of two gold stripes on the bottom of the samples. An additional antireflection (AR) coating is added to minimize reflection at the air/substrate interface. At room temperature 85-μm devices show a quantum efficiency of 5% at 1 mA and a maximum output power of 750 μW at 100 mA.

III. Experimental Results And Discussion

Fig. 1 shows the optical spectra of a 115-μm diameter device for three values of bias current: 1, 10, and 25 mA. The emission consists of a main peak centered at 1281.6 nm with a linewidth of approximately 18 nm and a secondary peak at 1225 nm. The main line shape is largely independent of bias. The spectrum of the main line is shown on a linear scale in the inset. It is clear at 25 mA there is an added spectral modulation on the line with a separation between peaks of this submodulation of 3 nm, which corresponds to an optical thickness of approximately 100 μm in InP. This implies that the substrate is acting as the spacer layer of a secondary Fabry–Perot.

A small-signal analysis has been carried out on 25-, 40-, 70-, and 115-μm diameter samples. No heat sink was used. A −5-dBm modulation power provided by the output of a 0.3–3000-MHz bandwidth network analyzer is superposed on a dc bias. This electrical signal is applied to the selected sample via a 20-GHz electrical probe. Emission is collected

1041–1135/99$10.00 © 1999 IEEE

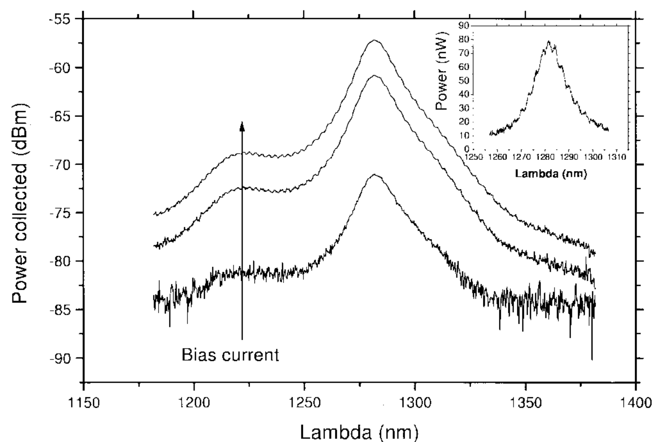

Fig. 1. Optical spectra plotted on a logarithmic scale for a 115-μm-diameter sample at 1, 20, and 25 mA. In the inset the scale is linear, for a bias of 25 mA.

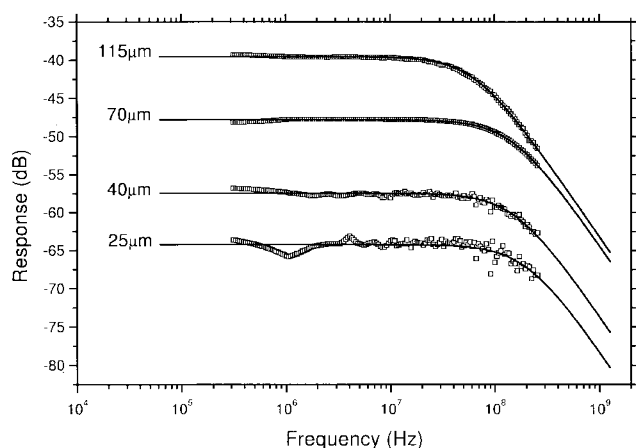

Fig. 2. Frequency response spectra (□) and fits (−) for four different MCLED diameters, each at a bias of 10 mA.

by a 62.5-μm diameter fiber butt-coupled to the substrate. The MCLED response is detected by a 6-GHz bandwidth photodiode. A 20-dB amplifier within the photodiode and an external 8-dB amplifier of 0.1–3-GHz bandwidth also amplify the electrical signal. This detected signal is returned to the input of the network analyzer. Acquisition is made using a resolution bandwidth of 3.7 kHz and 16 averages, which allows a minimum detection power of less than 4 nW.

A small signal analysis based on the rate equation applied to the case of MCLED's shows that the AM response of the MCLED can be described by the expression of a first-order low-pass filter transfer function

$$H(f) = \frac{H(0)}{\sqrt{1 + \left(\frac{f}{f_c}\right)^2}} \tag{1}$$

where f_c is the frequency at 3 dB. Typical measured frequency response spectra are shown in Fig. 2, for different size devices. For each of these experimental data curves, a fit based on (1) has been carried out, giving accurate values of $H(0)$ and f_c.

Fig. 3 presents the bandwidth of samples defined by the 3-dB cutoff frequency versus current density for several samples.

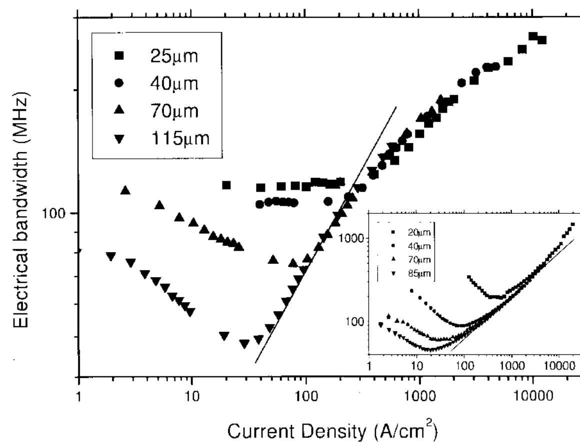

Fig. 3. 3-dB cutoff frequency as a function of current density for 25-, 40-, 70-, and 115-μm samples. The inset shows the 3-dB cutoff frequency as a function of current density for 20-, 40-, 70-, and 85-μm samples emitting at 990 nm. In both plots, the solid line represents bimolecular recombination, having a slope of 0.5.

For small diameter samples (<70 μm) the bandwidth is independent of the current density at low value. For larger samples in the range of 80–200 A/cm^2, a square-root law dependence is observed, characteristic of the bimolecular recombination process.

Above this range of current densities, the behavior of all samples deviates from that expected, presenting subsquare law dependence. To understand this behavior, it is worth considering the optical spectra presented in Fig. 1. With increasing current, a sidelobe appears at 1225 nm, caused by the radiative recombination of carriers within the DBR and/or barrier layers. Thus, an increase in bias does not necessarily result in an increase of the carrier density within the QW's, which is needed for a reduction of the carrier lifetime. To quantify the proportion of recombination within the QW to that in the barriers and the DBR layers, the following procedure is followed. To reach a BW of 200 MHz, for example, two current densities are identified, one calculated from the bimolecular process (solid line) and the other one from the measurement. Experimentally a current density of 2240 A/cm^2 is measured, whereas if the process was purely bimolecular with all carriers recombining in the wells, a current density of approximately 740 A/cm^2 would be required. The ratio between these densities, assuming only radiative recombination, is the proportion of carriers recombining in the QW's. This implies in the above case that only 33% of carriers are recombining in the QW when the injected current density is 2240 A/cm^2. At higher densities it is seen that the carrier confinement gets worse, dropping to around 10% at a density of 10 kA/cm^2. The origin of the leakage can be thermal, Auger processes and band-filling. At high densities, Auger recombination may increase the speed, as it is an additional recombination channel, however it may also increase the carrier leakage (and thus reduce the speed) due to the generation of high-energy electrons or holes that then escape from the well. The exact balancing between these simultaneous effects on modulation speed has not been calculated.

Below 80 A/cm^2, the behavior of the smaller sample does not present any obvious reduction of the 3-dB frequency with current density, like that of the bigger samples. At low bias densities and low frequency, the value of the diode impedance is high, but as the frequency is increased the impedance drops to a quasi-steady value. This characteristic at low biases implies that the modulation power injected into the device will not be constant as a function of frequency. Thus the impedance of the diode and not the recombination rate is found to determine the measured 3-dB value [14]. At high current densities, the impedance is low and fairly constant as a function of frequency, thus the modulation power of the sample is constant. The transfer function is then similar to that of a low-pass filter as it is determined by the recombination time of the carriers and not by an impedance effect. The inset of Fig. 3 shows the bandwidth of several diameter samples emitting at 990 nm versus current density; the structure of these samples is described in [13]. The current density dependence of the AM response presents some similarities with that of the 1.3 μm. We first observe a decrease of the 3-dB frequency due to some spurious impedance effects in the junctions explained previously. Above this minimum value, the bandwidth gets larger, with the increase of the current density following a square root dependence characteristic of a radiative recombination. A bandwidth of 1 GHz has been reached in these samples without saturation [15]. In both 1.3- and 990-nm MCLED's the band-filling inherent to the nature of the intrinsic material is present. However, it is clear that it does not drastically affect the performance of the 990-nm samples so we can conclude it does not play a key role in the bandwidth limitation of the 1.3-μm components. InGaAsP material is much more susceptible to Auger recombination than InGaAs one and particularly at high carrier density. The bandgap energies of wells and barriers of the 1.3-μm samples are 0.85 and 1.35 eV, respectively. The energy of 0.85 eV released during an electron–hole recombination event can be used by carriers in the well to be excited to higher energy levels in the band. If these energy levels are higher than 1.35 eV, carriers could escape from the well and recombine in the DBR layers and/or the barriers. From the above considerations it seems mostly likely that the bandwidth limitation in our samples are mainly due to a lack of carrier confinement. Efforts have to be made to improve this confinement through the use of new active material such as GaInNA's QW's or GaAs quantum dots.

IV. Conclusion

We have presented a small-signal analysis of MCLED's emitting at $\lambda = 1.3\,\mu$m. These samples showed an increase of the bandwidth with increasing current density. A bandwidth of 260 MHz has been achieved using a 25-μm diameter sample at 10 kA/cm^2. It seems that the onset of band filling of the QW's is achieved at low densities, around 200 A/cm^2. At higher densities the carriers are not so well confined to the QW regions. A small signal bandwidth of 1-GHz would be possible at a current density of 10 kA/cm^2 if ideal carrier confinement was achieved. Small signal bandwidths in excess of 1 GHz have been attained in MCLED's with good carrier confinement emitting at 990 nm.

References

[1] H. Yokoyama, K. Nish, T. Anan, Y. Nambu, S. Brorson, E. Ippen, and M. Sukuzi, "Controlling spontaneous emission and threshold-less laser oscillation with optical microcavities," *Opt. Quantum Electron.,* vol. 24, pp. S245–S272, 1992.

[2] A. Vredenberg, N. Hunt, E. Schubert, D. Jacobson, J. Poate, and G. Zydzik, "Controlled atomic spontaneous emission from Er^{+3} in a transparent Si/SiO_2 microcavity," *Phys. Rev. Lett.,* vol. 71, no. 4, pp. 517–520, 1993.

[3] G. Björk, S. Machida, Y. Yamamoto, and K. Igeta, "Modification of spontaneous emission rate in planar dielectric microcavity structures," *Phys. Rev. A,* vol. 44, no. 1, pp. 669–681, 1991.

[4] Z. Huang, C. Lin, and D. Deppe, "Spontaneous lifetime and quantum efficiency in light emitting diodes affected by a close metal mirror," *IEEE J. Quantum Electron.,* vol. 29, pp. 2940–2949, Dec. 1993.

[5] K. Streubel and R. Stevens, "High brightness (660nm) resonant cavity light-emitting diode," *IEEE Photon. Technol. Lett.,* vol. 10, pp. 1685–1685, Dec. 1998.

[6] U. Keller, G. Jacobovitz-Veselka, J. Cunningham, W. Jan, and B. Tell, "Microcavity enhanced vertical-cavity light emitting diodes," *Appl. Phys. Lett.,* vol. 62, no. 24, pp. 3085–3087, 1993.

[7] E. Hadji, J. Bleuse, N. Magnea, and J. Plautrat, "3.2μm infrared resonant cavity light emitting diode," *Appl. Phys. Lett.,* vol. 67, no. 18, pp. 2591–2593, 1995.

[8] K. Streubel and R. Stevens, "250Mbit/s plastic fiber transmission using 660nm resonant cavity light emitting diode," *Electron. Lett.,* vol. 34, no. 19, pp. 1862–1863, 1998.

[9] E. Schubert, N. Hunt, R. Malik, M. Micovic, and D. Miller, "Temperature and modulation characteristics of resonant-capacity light-emitting diodes," *J. Lightwave Technol.,* vol. 4, pp. 1721–1729, July 1996.

[10] N. Hunt, E. Schubert, R. Logan, and G. Zydzik, "Enhanced spectral power density and reduced linewidth at 1.3μm in InGaAsP quantum well resonant-cavity light emitting diode," *Appl. Phys. Lett.,* vol. 61, no. 19, pp. 2287–2289, 1992.

[11] M. Jalonen, M. T. J. Köngäs, P. Savolainen, S. Orsila, A. Salokatve, and M. Pessa, "Prospects of high efficient AlGaInP based surface emitting type ring-LED for 50 and 156 Mb/s POF data link systems," *Electron. Lett.,* vol. 34, no. 15, pp. 1519–1520, 1998.

[12] B. Depreter, S. Verstuyft, I. Moerman, R. Baets, and P. V. Daele, "InP-based microcavity LED's emitting at 1.3 μm and 1.55 μm," in *Proc. 11th Int. Conf. Indium Phosphide and Related Materials,* Davos, Switzerland, 1999, to be published .

[13] H. D. Neve, J. Blondelle, P. V. Vaele, P. Demeester, R. Baets, and G. Borghs, "Recycling of guided mode light emission in planar microcavity light emitting diodes," *Appl. Phys. Lett.,* vol. 70, no. 7, pp. 799–801, 1997.

[14] G. Shtengel, D. Ackerman, and P. Morton, "True carrier lifetime measurements of semiconductor lasers," *Electron. Lett.,* vol. 31, no. 20, pp. 1747–1748, 1995.

[15] B. Roycroft, A. Shaw, and J. Hegarty, "Dynamics of microcavity light emitters," presented at Photonics West, San Jose, CA, 1998.